

Supporting Information

Oxygen-rich hierarchical porous carbon nanosheets derived from KOH/KNO₃ co-activation treatment of soybean straw for high-performance supercapacitor

Yunxuan Li,^a Chuixiong Kong,^{a,c} Zurong Du,^{*b,d} Ju Zhang,^b Xuan Qin,^b Jiwei Zhang,^b Chulin Li,^b Yang Jin,^b and Shenggao Wang,^{*a}

a. Hubei Key Laboratory of Plasma Chemistry and Advanced Materials, Wuhan Institute of Technology, Wuhan 430073, PR China.

b. Hubei Key Laboratory of Automotive Power Train and Electronic Control, The college of Automotive Engineering, Hubei University of Automotive Technology, Shiyan 442002, PR China.

c. Department of Intelligent Manufacturing and Equipment, Guizhou Vocational Technology College of Electronics & Information, Kaili 556000, PR China.

d. Hubei Key Laboratory of Energy Storage and Power battery, and Collaborative Innovation Center for Optoelectronic Technology, Shiyan 442002, PR China. E-mail: dzr0227@163.com

Corresponding Authors:

Zurong Du, E-mail: dzr0227@163.com;

Shenggao Wang, E-mail: wyyysg@wit.edu.cn

1. Figures

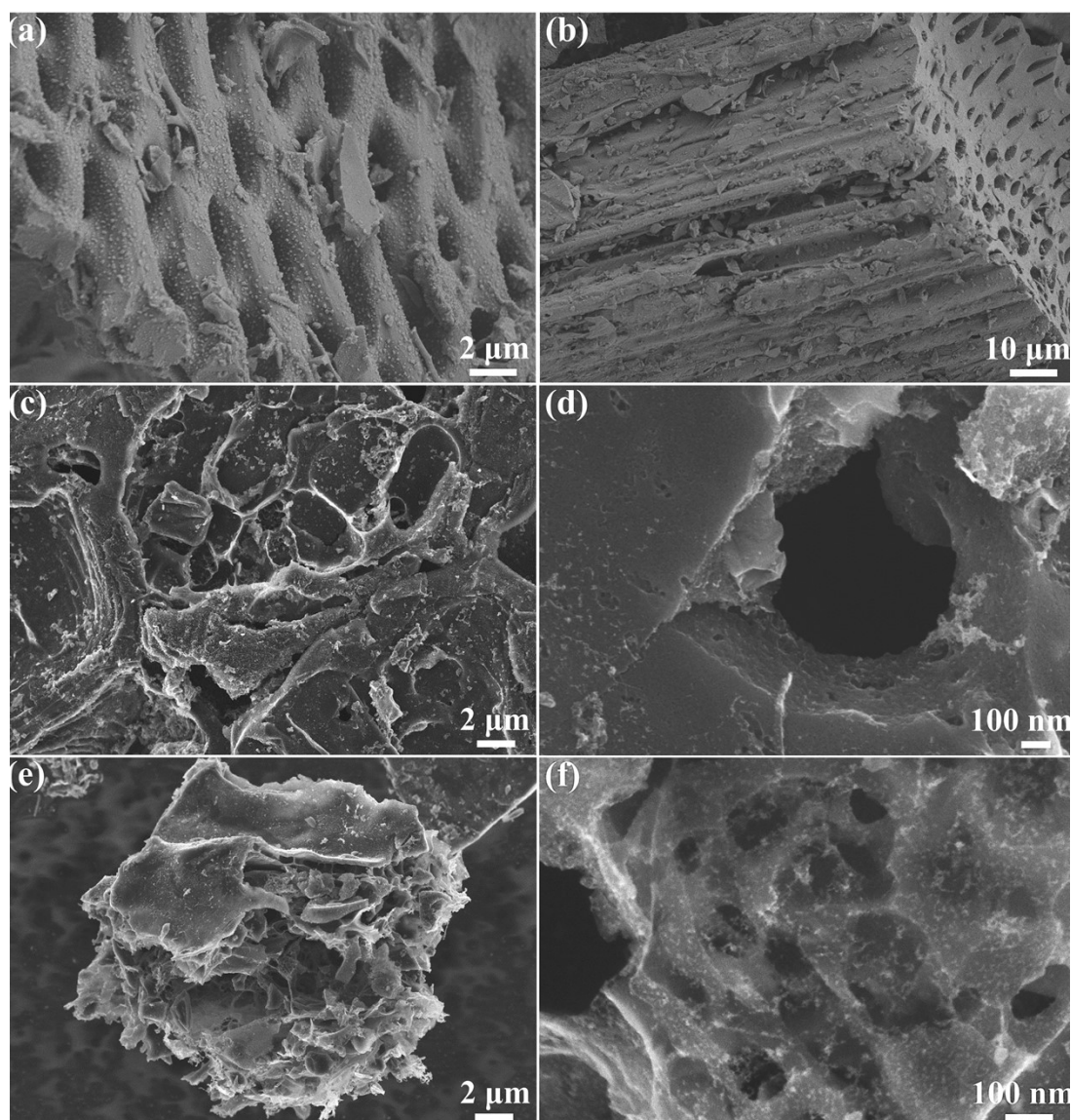


Figure S1 (a) and (b) the FE-SEM images of the carbonated sample SSC; (c) and (d) the FE-SEM images of the KOH/KNO₃ co-activated sample SSC2-0.5; (e) and (f) the FE-SEM images of the KOH/KNO₃ co-activated sample SSC2-0.7.

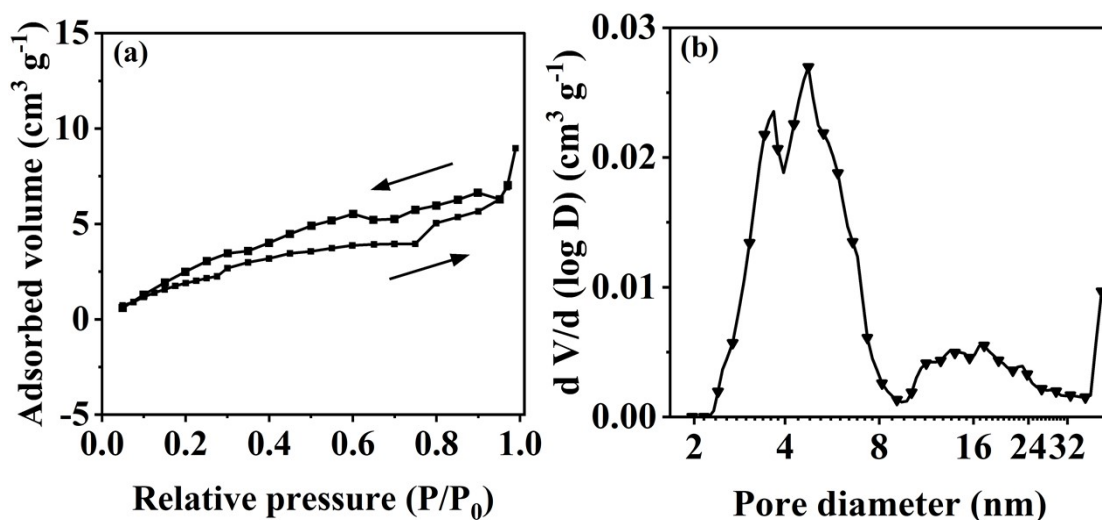


Figure S2 (a) N_2 adsorption-desorption isotherm of the carbonized sample SSC; (b) Pore size distribution of the carbonized sample SSC.

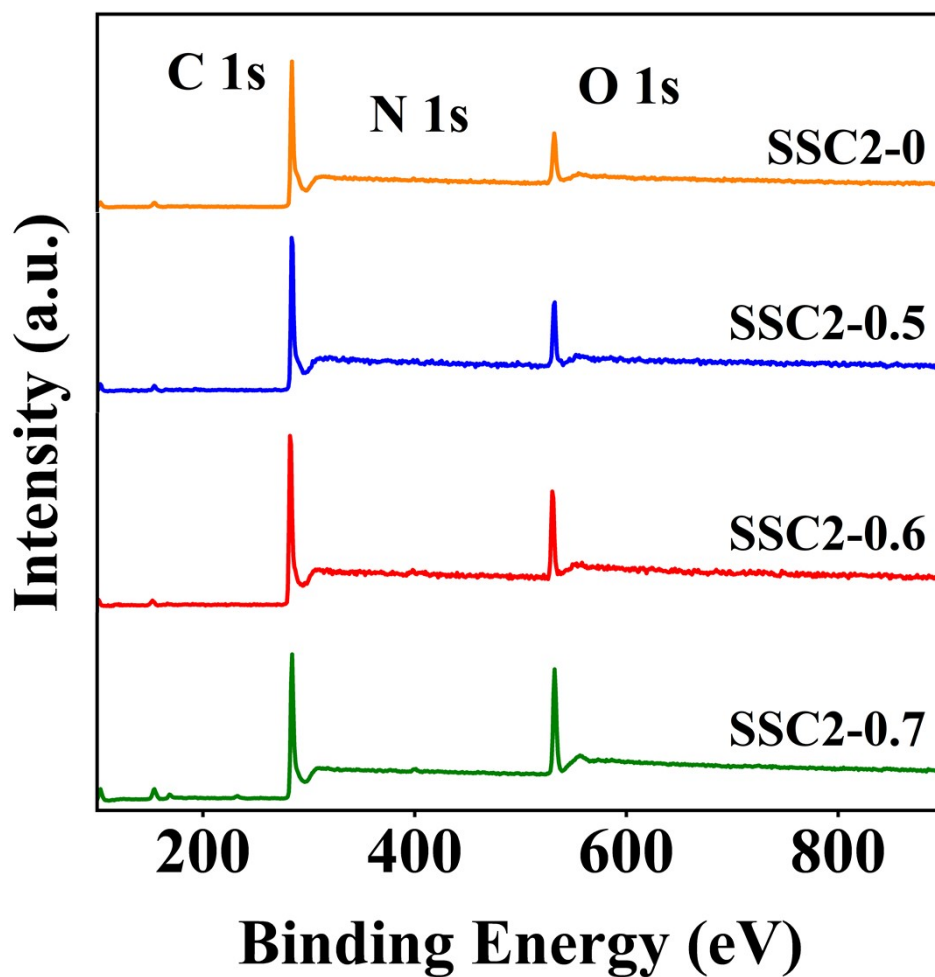


Figure S3 XPS spectra of the samples.

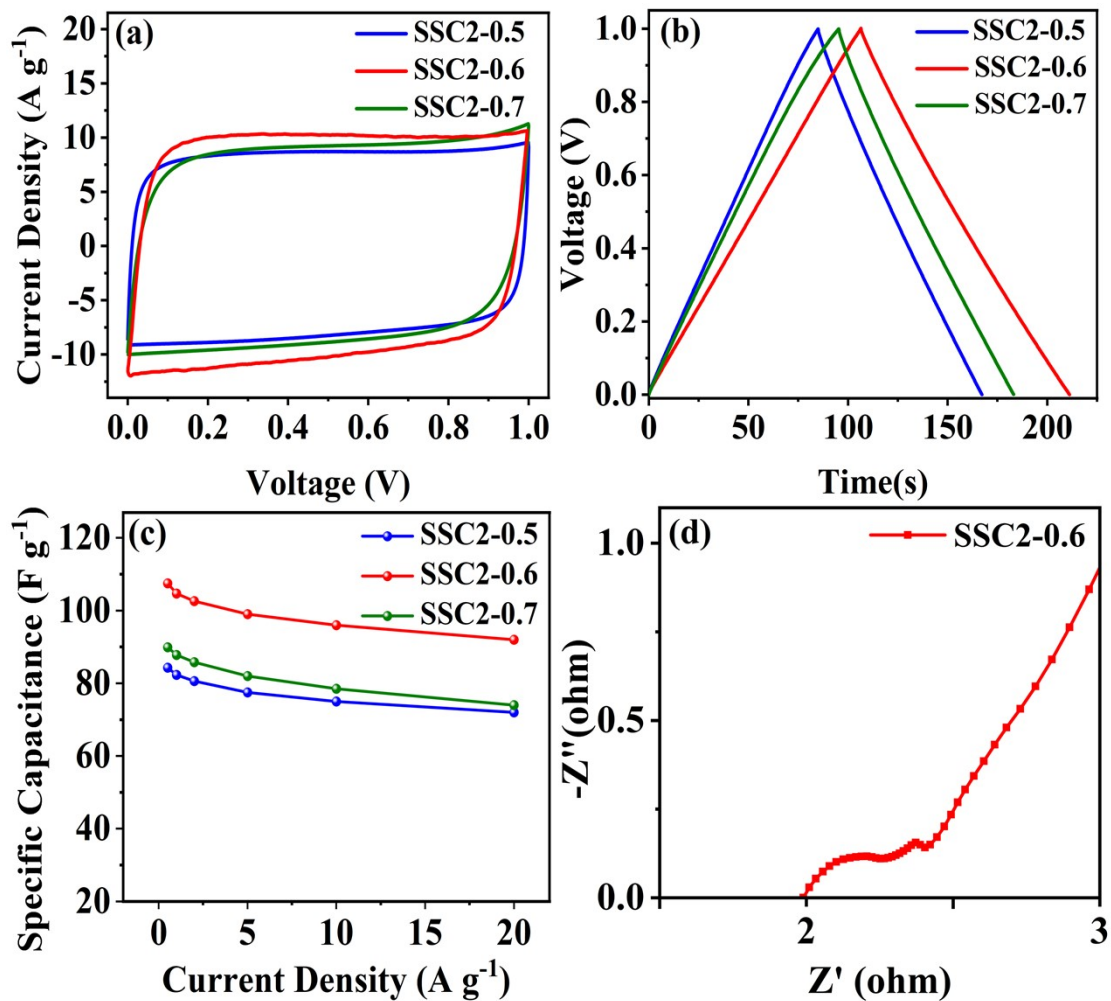


Figure S4 Capacitive properties of the symmetric supercapacitor: (a) CV curves at 100 mV s⁻¹; (b) GCD curves at 1 A g⁻¹; (c) the specific capacitances at different current density; (d) the enlarged plot of Figure 8 (d) at the high-frequency region.

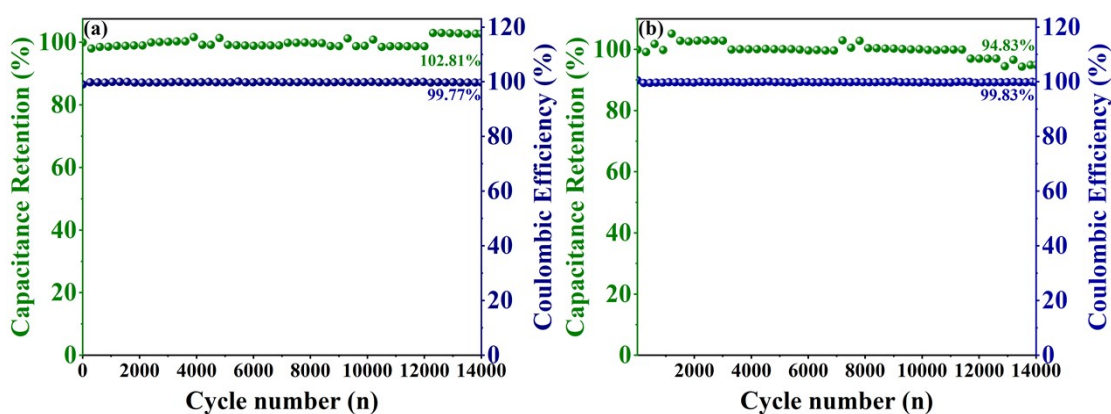


Figure S5 the stability of the capacitance retention and the coulombic efficiency of the samples with 14000 cycles at a current density of 10 A s⁻¹: (a) SSC2-0.5; (b) SSC2-0.7.

2. Tables

Table S1 The weight yield of the samples

Samples	before	after	Yield (%)	before	after	Yield (%)	Total yield (%)
	carbonization (g)	carbonization (g)		activation (g)	activation (g)		
SSC	10	2.7	27	/	/	/	/
SSC2-0	/	/	/	2	1.24	62	16.74
SSC2-0.5	/	/	/	2	1.08	54	14.58
SSC2-0.6	/	/	/	2	1.00	50	13.50
SSC2-0.7	/	/	/	2	0.96	48	12.96

Table S2 the elemental contents of the samples measured by the XPS.

sample	C (at.%)	O (at.%)	N (at.%)	the contents of carbon-containing functional groups (at.%)				the contents of oxygen-containing functional groups (at.%)			
				sp ² -C	sp ³ -C	C=O	O-C=O	C=O	C-OH	O-C=O	N-O
SSC2-0	86.98	11.83	1.19	53.80	19.40	8.36	5.42	0.57	9.27	1.16	0.83
SSC2-0.5	83.76	14.01	2.23	48.80	20.27	9.03	5.66	0.59	8.18	4.34	0.90
SSC2-0.6	80.88	16.77	2.35	42.31	20.86	11.70	6.01	0.97	7.23	7.38	1.19
SSC2-0.7	74.89	23.33	1.78	37.74	18.80	12.11	6.24	1.53	5.79	12.65	3.36

Table S3 The resistance values of the two-electrode system based on the equivalent circuit model.

samples	Resistance (Ω)		
	R_s	R_{ct}	Z_w
SSC2-0	4.57	10.73	5.03
SSC2-0.5	3.19	4.13	3.98
SSC2-0.6	3.63	3.40	2.14
SSC2-0.7	3.25	3.84	2.44

Table S4 Energy density vs. power density of the symmetric supercapacitor fabricated with the SSC2-0.6 electrode.

Current density (A g ⁻¹)	0.5	1	2	5	10	20
Energy density (Wh kg ⁻¹)	14.89	14.49	14.14	13.50	12.92	11.90
Power density (W kg ⁻¹)	249.44	498.22	992.28	2454.55	4845.00	9313.04